

Phenomenological study of Z' in the minimal B–L model at LHC

BALASUBRAMANIAM. K. M.^{1, 2, *}

¹ Department of Physics & Astronomy, University of Sussex, UK

² Theory Division, Physical Research Laboratory (PRL), India

*Corresponding author. E-mail: kmbala86@gmail.com

MS submitted on 6th Oct '16, for Pheno01@IISERM's Proceedings in Pramana - Journal of Physics.

Abstract. The phenomenological study of neutral heavy gauge boson (Z'_{B-L}) of the minimal B-L extension was done on the dimuon production channel of the LHC. The study begins with the LEP-II constraints on Z' searches, and the dimuon events are simulated at the parton level at the CM energies of 7 TeV and 8 TeV and studied with an integrated luminosity of 1.21 fb^{-1} and 20.5 fb^{-1} respectively. Later, the ATLAS detector-specific cuts unique to the Muon Pairs are imposed followed by the signal-selection-cuts on the Invariant Mass of the dimuon which restrict the events that are to be passed for Signal-Background Analysis, that are finally compared with the ATLAS data, and accounted for no experimental detection of Z'_{B-L} boson. It has been simulated further at the CM energy of 14 TeV with an integrated luminosity of 300 fb^{-1} to predict a possible discovery of this B-L neutral-heavy gauge boson with a mass corresponding to 1.5 TeV and a Z' coupling strength of 0.2 based on the signal-background analysis.

Keywords. Dataset-specific-parameters³, LEP-II constraints, Detector-specific-kinematic-cuts⁴, Signal-specific-kinematic-cuts⁵, Z'_{B-L} boson, heavy resonance, dimuon production channel, LHC, ATLAS.

PACS Nos 12.60.Cn; 12.60.Fr; 13.38.Dg; 13.85.Lg; 14.70.Hp; 14.70.Pw; 14.80.Bn; 14.80.Fd; 12.15.Ji; 11.80.Cr; 11.30.Fs

1. Introduction

The search on Z'_{B-L} is done on the dimuon production channel of the p-p LHC collisions, at the partonic level. The Drell Yan process, $p p \rightarrow \mu^+ \mu^-$ (upto tree level) are simulated in the B-L model, (intermediated by γ , Z , Z'_{B-L} , h_1 ¹ & h_2 ²) form the Signal-plus-Background, whereas in the SM process (intermediated by γ , Z & h ¹) forms the Background-alone. We have done the signal-background analysis in studying the potential for Z'_{B-L} discovery in the Large Hadron Collider (LHC).

1.1 Outline of the study

A brief introduction to the minimal B-L model is given in the following section (2.) covering the details on the $B - L$ Lagrangian (2.2) and the spontaneous breaking of the B-L symmetry with the gauge boson spectrum (2.3). In the third section (3.), the mechanics of this study are explained: starting from the Phenomenological tools (3.1) to the study of Z'_{B-L} confidence level

(CL) of a possible case (3.4.1) and ruling out the sisters' categories of the reviewed case by comparing with the ATLAS experimental bounds (3.4.2). Lastly, we conclude by making remarks on the studied cases (4.) and catch a glimpse of other experimentally ruled out cases (Figs. 6 - 10) that are involved in this research.

2. Theoretical Framework

2.1 The $B - L$ Model

The B-L model is a triply-minimal extension of the Standard Model (SM) in the gauge, scalar and fermion sectors. As the gauge sector of the SM is extended by a single U(1) factor related to Baryon minus Lepton (B-L) number, the $B - L$ gauge sector becomes minimal. Similarly, the requirement of a complex scalar singlet for Spontaneous Breaking of $B - L$ Symmetry makes the scalar sector as minimal. Thirdly, the introduction of an SM-singlet Right-Handed (RH) fermion per generation to eliminate the triangular $B - L$ gauge anomalies makes the fermion sector minimally extended. The B-L charge is chosen to cure the new gauge and mixed U(1) gravitational anomalies.

¹ SM Higgs

² $B - L$ Model Higgs

2.2 The Lagrangian of the minimal $B - L$ model

The Lagrangian of the minimal B-L Model obeying the $SU(3)_C \otimes SU(2)_L \otimes U(1)_Y \otimes U(1)_{B-L}$ gauge symmetry can be decomposed as:

$$\mathcal{L} = \mathcal{L}_S + \mathcal{L}_{YM} + \mathcal{L}_f + \mathcal{L}_Y \quad (1)$$

where the terms on the RHS are the scalar, Yang-Mills (YM)/gauge, fermion, and Yukawa parts respectively.

2.2.1 Scalar sector

For the spontaneous breaking of B-L symmetry of the extra $U(1)$ gauge group, a complex scalar singlet (χ) is introduced along with the SM scalar doublet (Φ). Thus the scalar Lagrangian becomes,

$$\mathcal{L}_S = (D^\mu \Phi)^\dagger (D_\mu \Phi) + (D^\mu \chi)^\dagger (D_\mu \chi) - V(\Phi, \chi)$$

with the scalar potential given by

$$\begin{aligned} V(\Phi, \chi) &= m^2 \Phi^\dagger \Phi + \mu^2 |\chi|^2 + \\ &\quad \left(\Phi^\dagger \Phi |\chi|^2 \right) \begin{pmatrix} \lambda_1 & \frac{\lambda_3}{2} \\ \frac{\lambda_3}{2} & \lambda_2 \end{pmatrix} \begin{pmatrix} \Phi^\dagger \Phi \\ |\chi|^2 \end{pmatrix} \\ &= m^2 \Phi^\dagger \Phi + \mu^2 |\chi|^2 + \lambda_1 (\Phi^\dagger \Phi)^2 + \\ &\quad \lambda_2 |\chi|^4 + \lambda_3 \Phi^\dagger \Phi |\chi|^2 \end{aligned}$$

where Φ and χ are the complex scalar Higgs doublet and singlet fields. For Φ and χ fields, the $B - L$ charges are taken as 0 and +2 respectively. The charge of the χ field has been chosen to ensure the gauge invariance of the fermions sector of the minimal $B - L$ model.

2.2.2 Yang-Mills / Gauge sector

The non-Abelian field strengths of this model are the same as in the SM whereas the Abelian ones can be written as follows:

$$\mathcal{L}_{YM}^{Abel} = -\frac{1}{4} F^{\mu\nu} F_{\mu\nu} - \frac{1}{4} F'^{\mu\nu} F'_{\mu\nu},$$

$$\begin{aligned} \text{where, } F_{\mu\nu} &= \partial_\mu B_\nu - \partial_\nu B_\mu, \\ F'_{\mu\nu} &= \partial_\mu B'_\nu - \partial_\nu B'_\mu \end{aligned}$$

The fields B_μ and B'_ν are the $U(1)_Y$ and $U(1)_{B-L}$ gauge fields respectively. In this field basis, the covariant derivative is

$$\begin{aligned} D_\mu &\equiv \partial_\mu + ig_S T^\alpha G_\mu^\alpha + ig T^\alpha W_\mu^\alpha \\ &\quad + ig_1 Y B_\mu + i(\tilde{g} Y + g'_1 Y_{B-L}) B'_\mu \end{aligned}$$

The gauge couplings \tilde{g} and g'_1 are free parameters. The pure $B - L$ model is defined by the condition $\tilde{g} = 0$ (i.e., the free parameter \tilde{g} is nullified at the EW scale). This implies no mixing at the tree level between the Z' bosons of $B - L$ Model and the Z bosons of the SM.

2.2.3 Fermion sector

The fermion Lagrangian density (with k being the generation index) is given by

$$\begin{aligned} \mathcal{L}_f &= \sum_{k=1}^3 \left(i\bar{q}_{kL} \gamma_\mu D^\mu q_{kL} + i\bar{q}_{kR} \gamma_\mu D^\mu q_{kR} + \right. \\ &\quad i\bar{d}_{kR} \gamma_\mu D^\mu d_{kR} + i\bar{l}_{kL} \gamma_\mu D^\mu l_{kL} + \\ &\quad \left. i\bar{e}_{kR} \gamma_\mu D^\mu e_{kR} + i\bar{\nu}_{kR} \gamma_\mu D^\mu \nu_{kR} \right) \end{aligned}$$

where the fields' charges are the usual SM and $B - L$ ones (in particular, $B - L = \frac{1}{3}$ for quarks and -1 for leptons with no distinction between generations, hence ensuring universality). The $B - L$ charge assignments of the fields as well as the introduction of new fermion RH heavy neutrinos (ν_R 's, charged -1 under $B - L$) are designed to eliminate the triangular $B - L$ gauge anomalies of the theory.

Therefore, the $B - L$ gauge extension of the SM gauge group broken at the TeV scale necessarily requires at least one new scalar field and three new fermion fields which are charged with respect to the $B - L$ group.

2.2.4 Yukawa sector

Finally, the Yukawa interactions are

$$\begin{aligned} \mathcal{L}_Y &= \sum_{i,j,k=1}^3 -y_{jk}^d \bar{q}_{jL} d_{kR} \Phi - y_{jk}^u \bar{q}_{jL} u_{kR} \tilde{\Phi} \\ &\quad - y_{jk}^e \bar{l}_{jL} e_{kR} \Phi - y_{jk}^\nu \bar{l}_{jL} \nu_{kR} \tilde{\Phi} \\ &\quad - y_{jk}^M (\bar{\nu}_R)_j^c \nu_{kR} \chi + h.c. \end{aligned}$$

where $\tilde{\Phi} = i\sigma^2 \Phi^*$ and the last term is the Majorana contribution, and the others are the usual Dirac ones. While working on the basis in which the RH neutrino Yukawa coupling matrices, y^M are diagonal, real, and positive, these are the only allowed gauge invariant terms. The last term in the above equation combines the neutrinos to the new scalar singlet field, χ , which allows the dynamical generation of neutrino masses, and acquires a VEV through the Higgs mechanism.

2.3 Spontaneous breaking of $B - L$ Symmetry & gauge boson spectrum

In the Feynman gauge, the scalar fields (Φ & χ) can be parametrized [1] as

$$\begin{aligned} \Phi &= \frac{1}{2} \begin{pmatrix} -i(\omega^1 - i\omega^2) \\ \nu + (h + iz) \end{pmatrix} \\ \chi &= \frac{1}{\sqrt{2}} (x + (h' + iz')) \end{aligned}$$

where $\omega^\pm = \omega^1 \mp i\omega^2$, z & z' are the would-be Goldstone bosons of W^\pm , Z and Z' respectively.

$$D^\mu \Phi (D_\mu \Phi)^\dagger = \frac{1}{2}(\partial^\mu h)(\partial_\mu h) + \frac{1}{8}(h + v)^2 \left[g^2 |W_1^\mu|^2 - iW_2^\mu|^2 + (gW_3^\mu - g_1 B^\mu - \tilde{g} B'^\mu)^2 \right]$$

and

$$D^\mu \chi (D_\mu \chi)^\dagger = \frac{1}{2}(\partial^\mu h')(\partial_\mu h') + \frac{1}{2}(h' + x)^2 (g'_1 2B'^\mu)^2$$

where we have taken $Y_\chi^{B-L} = 2$ to guarantee the gauge invariance of the Yukawa terms (2.2.4). In the first of the above two equations, we can recognise immediately the SM charged gauge bosons W^\pm , with $M_W = \frac{g v}{2}$ as in the SM. The other gauge boson masses are not so simple to identify, because of mixing. In analogy with the SM, the fields of definite mass are linear combinations of B^μ , W_3^μ and B'^μ . The explicit expressions are:

$$\begin{pmatrix} B^\mu \\ W_3^\mu \\ B'^\mu \end{pmatrix} = X \begin{pmatrix} A^\mu \\ Z^\mu \\ Z'^\mu \end{pmatrix}$$

where,

$$X = \begin{pmatrix} \cos\vartheta_\omega & -\sin\vartheta_\omega \cos\vartheta' & \sin\vartheta_\omega \sin\vartheta' \\ \sin\vartheta_\omega & \cos\vartheta_\omega \cos\vartheta' & -\cos\vartheta_\omega \sin\vartheta' \\ 0 & \sin\vartheta' & \cos\vartheta' \end{pmatrix}$$

with $-\frac{\pi}{4} \leq \vartheta' \leq \frac{\pi}{4}$, such that:

$$\tan 2\vartheta' = \frac{2\tilde{g} \sqrt{g^2 + g_1^2}}{\tilde{g}^2 + 16(\frac{x}{v})^2 g_1'^2 - g^2 - g_1^2}$$

The gauge boson masses are:

$$M_A = 0 \quad (2)$$

Now, setting \tilde{g} to 0 for the pure $B-L$ model, the mixing angle ϑ' vanishes, implying no mixing, at the tree level, between the Z_{SM} and Z'_{B-L} bosons. The Z and Z'_{B-L} masses are:

$$M_Z = \sqrt{g^2 + g_1^2} \frac{v}{2}, \quad (3)$$

$$M_{Z'_{B-L}} = 2g'_1 x \quad (4)$$

To complement the section on the $B-L$ model, we summarise the mass eigenstates and the assignation of Hypercharge (Y) and B-L quantum number ($B-L$) to the chiral fermionic and scalar fields in Tables 1 & 2 respectively.

Name	Quarks	Leptons	Neutrinos	Higgses
ψ	q	l	ν_l & ν_h	h_1 & h_2
Mass	m_q	m_l	m_{ν_l} & m_{ν_h}	m_{h_1} & m_{h_2}

Table 1: Mass eigenstates [1]

ψ	q_L	u_R	d_R	l_L	e_R	ν_R	Φ	χ
$SU(3)_C$	3	3	3	1	1	1	1	1
$SU(2)_L$	2	1	1	2	1	1	2	1
Y	$\frac{1}{6}$	$\frac{2}{3}$	$-\frac{1}{3}$	$-\frac{1}{2}$	-1	0	$\frac{1}{2}$	0
$B-L$	$\frac{1}{3}$	$\frac{1}{3}$	$\frac{1}{3}$	-1	-1	-1	0	2

Table 2: Hypercharge (Y) and $B-L$ quantum number assignation to chiral fermion and scalar fields [1].

3. Z'_{B-L} - Analysis & Results

3.1 Phenomenological Tools

The search for Z'_{B-L} boson is done on the dimuon production channel of the LHC process, $p p \rightarrow \mu^+ \mu^-$. We have taken the FeynRules model file for the Minimal $B-L$ model, implemented by L. Basso and G. M. Pruna [2]. The motivation was to get myself introduced to the techniques of FeynRules [19]. We used FeynRules2.0 [20] and Mathematica (version - 9) [5] to generate the Universal FeynRules Output (UFO) [22] files which were fed into the event generator, MadGraph5.0 [3]. We have used the inbuilt Parton Density Function (PDF) set, CTEQ6L1 in MadGraph5.0 [3] for our study. We have resorted to the standard Large Electron Positron (LEP)-II bounds [8] on Z' searches as shown in Fig. 1 to standardise the values of the parameters for our study.

3.2 Initialisation of Z'_{B-L} Parameters

We have chosen the values of Z' coupling constant (g'_1)³ as 0.2 and 0.5 with four different mass ($M_{Z'}$ in TeV)³ parameters of values: 1.5, 2.0, 3.0, and 5.0 respectively in accordance with the bounds from the LEP-II exper-

³Dataset-specific-parameters: Z' -Prime's coupling constant (g'_1), mass ($M_{Z'}$), and total decay width ($\Gamma_{Z'}$).

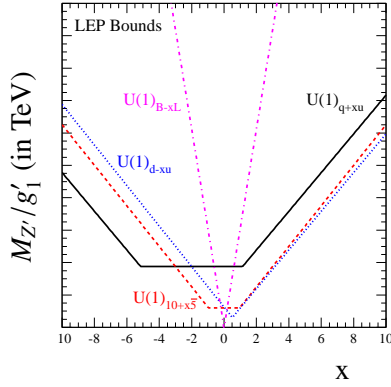


Figure 1: LEP-II constraints [8] on $\frac{M_{Z'}}{g'_1}$ of various Z' models. For the value of $x=1$ (i.e., for B-L Model), only $\frac{M_{Z'}}{g'_1} \geq 6$ TeV are allowed.

iment. The expression for the partial decay widths ($\Gamma_{Z' \rightarrow f\bar{f}}$) of Z'_{B-L} into SM fermions has been derived from the coupling vertex of Z'_{B-L} with the SM fermions is:

$$\Gamma_{Z' \rightarrow f\bar{f}} = \frac{M_{Z'}}{12\pi} C_f (v^f)^2 \left[1 + 2 \frac{m_f^2}{M_{Z'}^2} \right] \sqrt{1 - \frac{4m_f^2}{M_{Z'}^2}}$$

where, C_f is the color-factor of the fermion (f), $v^f (= (B-L) g'_1)$, is the coupling between the $B-L$ charge of fermion (f) and Z' coupling b/w SM fermions (g'_1) and m_f is the mass of fermion (f). The total decay width ($\Gamma_{Z'}$)³ of Z'_{B-L} boson is the sum of all the partial decay widths ($\Gamma_{Z' \rightarrow f\bar{f}}$) of Z'_{B-L} into SM-fermion pairs except the neutrino-pairs (taking the SM-neutrinos as massless). These set of parameters are grouped into six datasets as shown in Table 3.

Initially, the $B-L$ model (in the form of UFO [22] files) has been imported in the MadGraph5.0's [3] environment and the process $p p \rightarrow \mu^+ \mu^-$ is generated. Then, the dataset-specific-parameters³ are set in the created process directory to produce 1 million partonic-level events at the Centre of Mass (CM) energy of 7 TeV, per each Invariant-Mass (of charged lepton pairs) window of varied sizes. These windows are to ensure no loss of any significant events across the whole range of simulation which has spanned across the entire Invariant Mass range of 0 - 7000 GeV of the final state Muon pairs. The simulated events' format in compliant with the Les Houches Event Accord (LHEA) [23] was generated as the Les Houches Event (LHE) [23] files.

These event files (LHE) corresponding to each Invariant Mass window were fed into MadAnalysis5 [21] where they got joined into a single large LHE [23] file. Corresponding to a particular dataset, which encom-

	0.2	0.5	g'_1
1500	38.20 A	nil ^a	$\Gamma_{Z'}$ (in GeV)
2000	50.93 B	nil ^a	$\Gamma_{Z'}$ (in GeV)
3000	76.39 C	477.45 D	$\Gamma_{Z'}$ (in GeV)
5000	127.32 E	795.75 F	$\Gamma_{Z'}$ (in GeV)
$M_{Z'}$ (in GeV)			

where,
 [C] : the Z' signal with $M_{Z'} = 3000$ GeV, $g'_1 = 0.2$ and $\Gamma_{Z'} = 76.39$ GeV

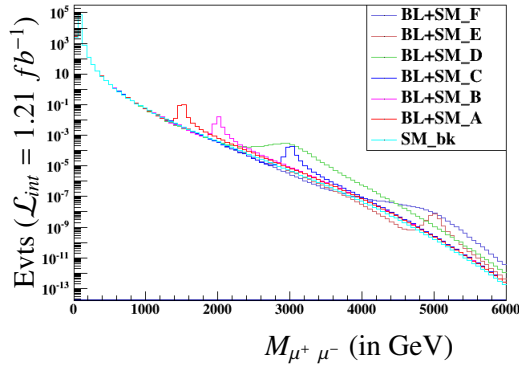
Table 3: The datasets with different values of 3 parameters viz., mass ($M_{Z'}$), coupling of Z'_{B-L} with SM Fermions (g'_1) and the total decay width of Z'_{B-L} into SM Fermions ($\Gamma_{Z'}$) upon which this study is based.

^a The datasets corresponding to the parameters $g'_1 = 0.5$ with $M_{Z'} = 1.5$ & 2.0 TeV are discarded as the LHE files corresponding to them got corrupted.

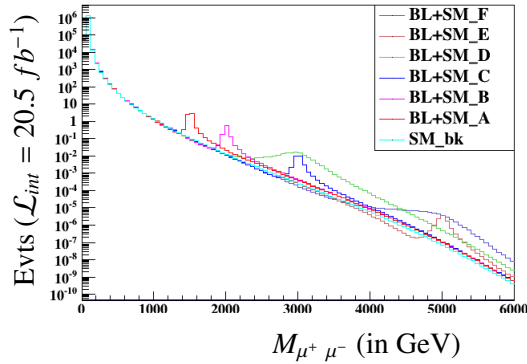
passes the entire simulation range of width approximately 6000 - 7000 GeV of Muon Pairs' Invariant Mass.

3.3 Comparison of 7, 8 & 14 TeV simulated events of all the datasets

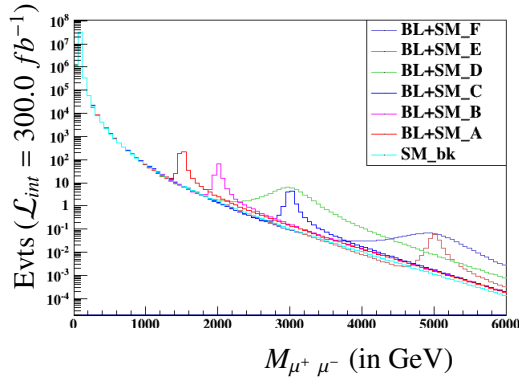
At this juncture, the obtained single LHE file of massive size was normalised with an integrated luminosity of 1.21 fb^{-1} . The whole machinery of section (3.1) was repeated for the remaining datasets. All of these datasets are an admixture of Z'_{B-L} signal and the SM background. For the analysis of Z'_{B-L} signal from the background, another LHE file of large size has been generated as previously for the SM process. This generation was done by importing the default model SM in the MG5 environment and simulated the events for the dimuon production from proton-proton collisions with the same PDF set, CTEQ6L1.



(a) Simulated events at 7 TeV CM energies.



(b) Simulated events at 8 TeV CM energies.



(c) Simulated events at 14 TeV CM energies.

Figure 2: Z'_{B-L} Resonances in the process, $p p \rightarrow \mu^+ \mu^-$ for considered datasets (signal + bkgrd) and dataset - SM (bkgrd alone) without any Kinematic Cuts. The events-distributions of all the seven datasets are super-imposed one upon other. The resonance of the SM's Z boson at $M_{\mu^+ \mu^-} = 91.18$ GeV can be seen very close to 0 GeV of $M_{\mu^+ \mu^-}$.

The distribution of Events versus the Muon Pairs' Invariant mass is shown in Figure 2a at the CM energy of 7 TeV with an integrated luminosity of $\mathcal{L}_{int} = 1.21$

fb^{-1} . We have repeated the similar study with the collision energy of 8 TeV and 14 TeV and normalised the generated partonic-level events with an integrated luminosity of $\mathcal{L}_{int} = 20.5 fb^{-1}$ and $\mathcal{L}_{int} = 300.0 fb^{-1}$ respectively. The events distribution with the Muon Pairs' Invariant mass for the two cases just discussed is shown in Figures 2b and 2c.

We shall observe an increase in the total number of events as we move from the Events Distributions studied at the CM energies of 7 TeV to 8 TeV and then to 14 TeV respectively. The events distributions corresponding to all the datasets are colour coded distinctly in all the detailed figures. The signal peaks become prominent with increasing collision energy and integrated luminosity, which is very conspicuous in the Figures 2a, 2b and 2c. This variation in the signal's prominence shall be accounted for a potential discovery of Z'_{B-L} in the upcoming sections.

The events distributions shown in Fig. 2 have six Z'_{B-L} signal peaks corresponding to the Signal-plus-Background-datasets, and one peak at $M_{\mu^+ \mu^-} = 91.18$ GeV corresponding the SM Z-resonance where the six Signal-plus-Background datasets (viz., A, B, C, D, E & F) coincide with Background-Alone dataset (dataset - SM).

3.4 Signal Vs Background Analysis for Z'_{B-L} Resonance in Datasets - A & SM

The LHE files of dataset - A and the dataset - SM generated at 7 TeV CM energy were fed into MadAnalysis5 [21] environment and normalised to an integrated luminosity of $\mathcal{L}_{int} = 1.21 fb^{-1}$.

Then, two detector-specific-kinematic-cuts⁴ were applied on the transverse momenta ($P_T > 20.0$ GeV)⁴ and Pseudorapidity ($\eta < 2.4$)⁴ of the final state Muon Pairs and the events satisfying these cuts were selected for further study. We have calculated the cumulative efficiency (which is a ratio between the selected events and the sum of selected & rejected events) after the cuts and checked that it's never greater than 1, to ensure that we didn't lose any significant events with these cuts.

The signal-specific-kinematic-cuts⁵ (common for studies done at 7, 8 & 14 TeV CM energies.) on the In-

⁴ (ATLAS) Detector-specific-kinematic-cuts on final state Muon Pairs: $P_T > 20.0$ GeV and $\eta < 2.4$ (common to all the datasets).

⁵ Signal-specific-kinematic-cuts on $M_{\mu^+ \mu^-}$ of Datasets (with Sgnl+Bkgrd) :

$692.7 \text{ GeV} \leq M_{\mu^+ \mu^-} \leq 2307.3 \text{ GeV}$ (for $\Gamma_{SW}^{signal-A}$)

$923.6 \text{ GeV} \leq M_{\mu^+ \mu^-} \leq 3076.4 \text{ GeV}$ (for $\Gamma_{SW}^{signal-B}$)

$1385.4 \text{ GeV} \leq M_{\mu^+ \mu^-} \leq 4614.6 \text{ GeV}$ (for $\Gamma_{SW}^{signal-C}$)

$783.8 \text{ GeV} \leq M_{\mu^+ \mu^-} \leq 5216.2 \text{ GeV}$ (for $\Gamma_{SW}^{signal-D}$)

$2309.0 \text{ GeV} \leq M_{\mu^+ \mu^-} \leq 7691.0 \text{ GeV}$ (for $\Gamma_{SW}^{signal-E}$)

$1306.4 \text{ GeV} \leq M_{\mu^+ \mu^-} \leq 8693.6 \text{ GeV}$ (for $\Gamma_{SW}^{signal-F}$)

(same for datasets at 7, 8 & 14 TeV collision energies.)

variant Mass ($M_{\mu^+ \mu^-}$) have been chosen as a Sampling Window (SW) with width (Γ_{SW}) is:

$$\Gamma_{SW}^{signl-A} = M_{Z'}^{signl-A} \pm 3 \Gamma_{Z'}^{signl-A} \quad (5)$$

Thus, for dataset - A, with $M_{Z'}^{signl-A} = 1500$ GeV & $\Gamma_{Z'}^{signl-A} = 38.20$ GeV, the signal-specific-cuts can be implemented by selecting the events whose invariant mass falls within the range,

$$692.7 \text{ GeV} \leq M_{\mu^+ \mu^-} \leq 2307.3 \text{ GeV} \text{ (for } \Gamma_{SW}^{signl-A} \text{)}$$

The event distribution with the Muon Pairs' invariant mass for dataset - A, at 7 TeV Collision energy is shown in Figure 4a. By repeating the formerly mentioned procedures, the event distributions for dataset - A, at 8 TeV & 14 TeV were obtained which are shown in Fig. 5a and Fig. 3 respectively.

The Confidence Level (CL) / statistical significance of the Z'_{B-L} signal has been calculated using:

$$K_{Signal} = K_A - K_{SM}$$

$$Signal's \text{ CL} = \frac{K_{Signal}}{\sqrt{K_{Signal} + K_{Bkgnd}}}$$

3.4.1 Confidence Level of Signal in dataset - A at 14 TeV collision energy

We have studied the confidence level of Z'_{B-L} signal of the dataset - A at 14 TeV with an integrated luminosity of $\mathcal{L}_{int} = 300 \text{ fb}^{-1}$. The events distributions with the invariant mass for datasets - A & SM at 14 TeV CM energy are shown in Fig. 3. The number of events selected for Signal-Background analysis after the application of three successive kinematic cuts on the datasets that are just discussed, in the same order is listed in Table 4.

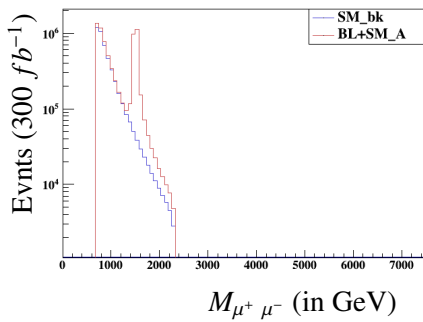


Figure 3: Events distributions for datasets - A & SM at 14 TeV after cuts on P_T , η , & M with Z'_{B-L} signal with CL of 9.5σ at $M_{\mu^+ \mu^-} = 1.5$ TeV ($M_{Z'}^{dataset-A}$) & $g'_1 = 0.2$.

Data Set - A (Signal + Back-ground)	Events Retained $K \pm \delta K$	Events Rejected $R \pm \delta R$
No cut	35351789 \pm 10184.5	nil
$P_T > 20.0$ GeV	26308333 \pm 9352	9043456 \pm 4033
$\eta < 2.4$	26294016 \pm 9348	14317 \pm 119
692.7 GeV < M < 2307.3 GeV	1126.2 \pm 33.6	26292890 \pm 9347
Data Set - SM (Background Alone)	Events Retained $K \pm \delta K$	Events Rejected $R \pm \delta R$
No cut	35527829 \pm 10662.1	nil
$P_T > 20.0$ GeV	26949438 \pm 9895	8578391 \pm 3971
$\eta < 2.4$	26935139 \pm 9890	14298 \pm 119
692.7 GeV < M < 2307.3 GeV	807.6 \pm 28.4	26934331 \pm 9890

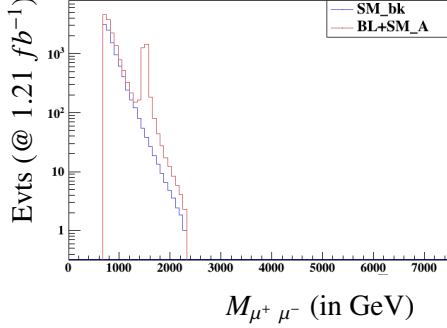
Table 4: Selected and Rejected Events after the kinematic cuts on final state muon pairs for the datasets - A & SM at 14 TeV p-p Collisions

The CL of Z'_{B-L} signal has been calculated to be 9σ which accounts for a possible experimental discovery.

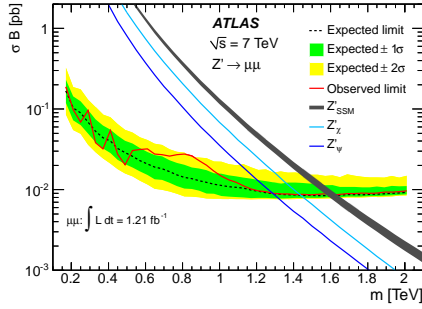
3.4.2 Comparison of datasets - A & SM at 7 and 8 TeV collisions with respective ATLAS Results

The dataset - A studied at 7 TeV collision energy has been compared with the ATLAS experimental bounds on the searches of Z' in the dimuon channel at 7 TeV LHC collisions with an integrated luminosity (\mathcal{L}_{int}) of 1.21 fb^{-1} [24]. The CL of the signal in the dataset - A, at 7 TeV collision is 0.1σ , which is merely a statistical fluctuation as shown in Fig. 4a. We have confirmed with the ATLAS results of 7 TeV p-p collisions at 1.5 TeV where the cross section is continuous with

no signal-peak, corresponding to the solid red line, titled “Observed limit” in Fig. 4b.



(a) Events distribution of datasets - A & SM at 7 TeV collisions with Z'_{B-L} signal of 0.1σ significance.



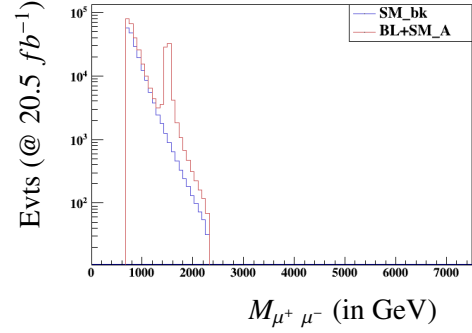
(b) Variation of cross section with invariant mass - ATLAS searches on Z' in dimuon production channel at 7 TeV [24] Collisions with an integrated luminosity (\mathcal{L}_{int}) of 1.21 fb^{-1} with no singularity at $M_{\mu^+\mu^-} = 1.5 \text{ TeV}$.

Figure 4: Comparison between datasets - A & SM with ATLAS searches on the neutral heavy resonance at 7 TeV p-p collisions with an integrated luminosity (\mathcal{L}_{int}) of 1.21 fb^{-1} .

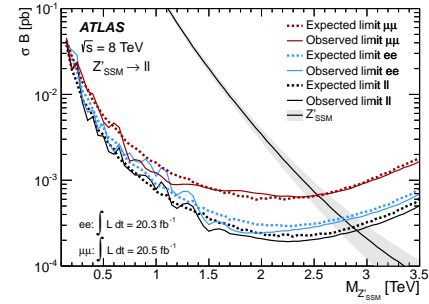
A similar comparison between Figures 5a & 5b has been made to confirm the Z'_{B-L} resonance with CL of 0.8σ in the dataset - A, at 8 TeV p-p collision corresponds to no experimental possibility. This detection impossibility is indicated by the continuous solid red line without any singularity, captioned with “Observed limit $\mu\mu$ ” in Fig. 5b [25].

4. Conclusion

Thus with the signal significance (CL) of 9σ for dataset - A at 14 TeV CM energy with $\mathcal{L}_{int} = 300 \text{ fb}^{-1}$, this study predicts a potential discovery of the heavy neutral gauge boson (Z'_{B-L}) corresponding to the dataset - A with a mass $M_{Z'}$ of 1.5 TeV and a Z' coupling strength g'_1 of 0.2 with the SM-fermions at the LHC as in Fig. 3.



(a) Events distribution for datasets - A & SM at 8 TeV collisions with the Z'_{B-L} signal of 0.8σ significance.



(b) Variation of cross section with invariant mass - ATLAS searches on Z' in dimuon production channel at 8 TeV [25] Collisions with an integrated luminosity (\mathcal{L}_{int}) of 20.5 fb^{-1} with no resonance at $M_{\mu^+\mu^-} = 1.5 \text{ TeV}$.

Figure 5: Comparison between datasets - A & SM with ATLAS searches on the neutral heavy resonance at 8 TeV p-p collisions with an integrated luminosity (\mathcal{L}_{int}) of 20.5 fb^{-1} .

The comparative study between the datasets - A & SM with the ATLAS experimental searches on heavy resonances at 7 and 8 TeV on the dimuon channel confirms the non-observance of any Z' boson. And this comparison validates our study of Z'_{B-L} signal with CL of 0.1σ and 0.8σ at 7 and 8 TeV collisions of datasets - A & SM respectively as in Figs. 4 & 5.

Appendix A. Comparison of 7, 8 & 14 TeV simulated datasets

The event distribution of the remaining datasets with Muon Pairs' Invariant mass, studied at 7, 8 & 14 TeV are compared in this appendix (Figs. 6, 7, 8, 9 & 10 corresponding to datasets - B, C, D, E, & F respectively). In all these cases, the CL of Z'_{B-L} signal is less than 3σ , which are accounted for no experimental discoveries.

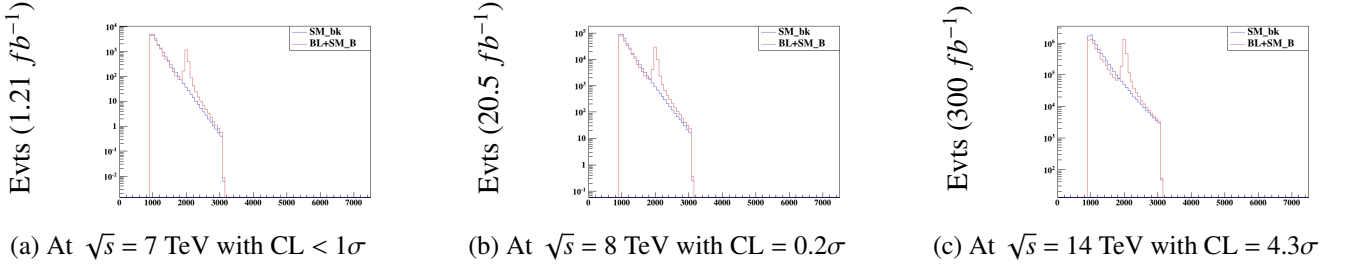


Figure 6: Dataset - B with cuts, P_T^4 , η^4 and $923.6 \text{ GeV} \leq M_{\mu^+ \mu^-} \leq 3076.4 \text{ GeV}$ (for $\Gamma_{SW}^{signl-B}$)⁵

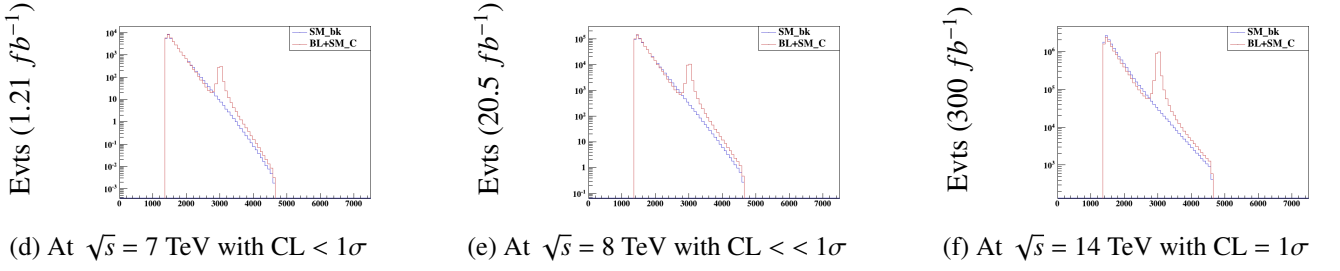


Figure 7: Dataset - C with cuts, P_T^4 , η^4 and $1385.4 \text{ GeV} \leq M_{\mu^+ \mu^-} \leq 4614.6 \text{ GeV}$ (for $\Gamma_{SW}^{signl-C}$)⁵

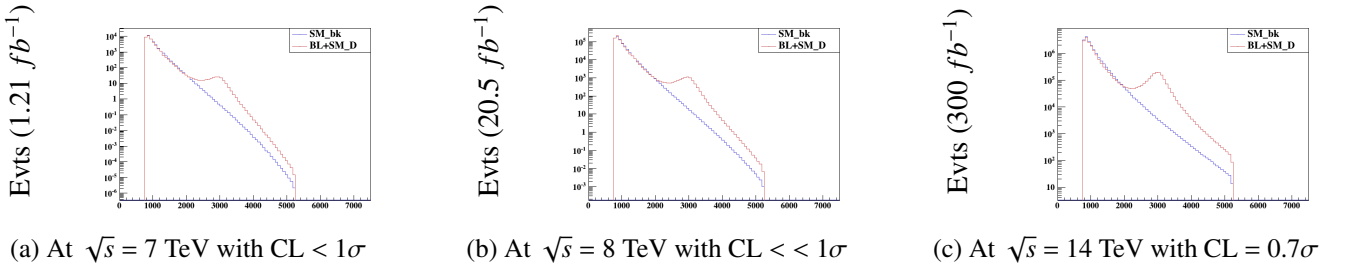


Figure 8: Dataset - D with cuts, P_T^4 , η^4 and $783.8 \text{ GeV} \leq M_{\mu^+ \mu^-} \leq 5216.2 \text{ GeV}$ (for $\Gamma_{SW}^{signl-D}$)⁵

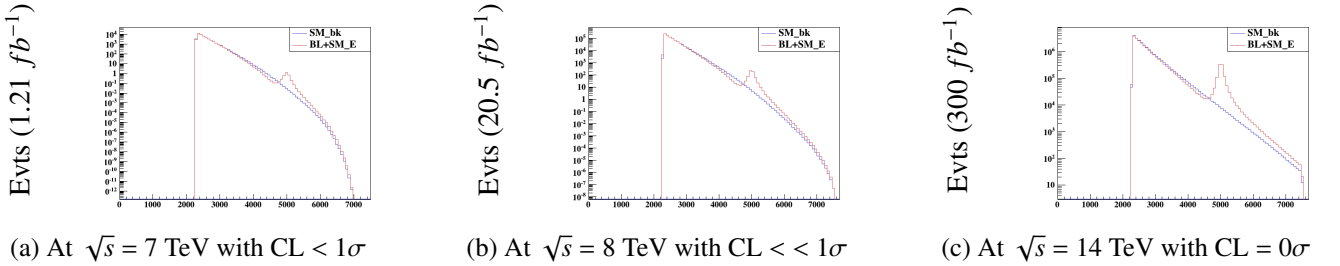


Figure 9: Dataset - E with cuts, P_T^4 , η^4 and $2309.0 \text{ GeV} \leq M_{\mu^+ \mu^-} \leq 7691.0 \text{ GeV}$ (for $\Gamma_{SW}^{signl-E}$)⁵

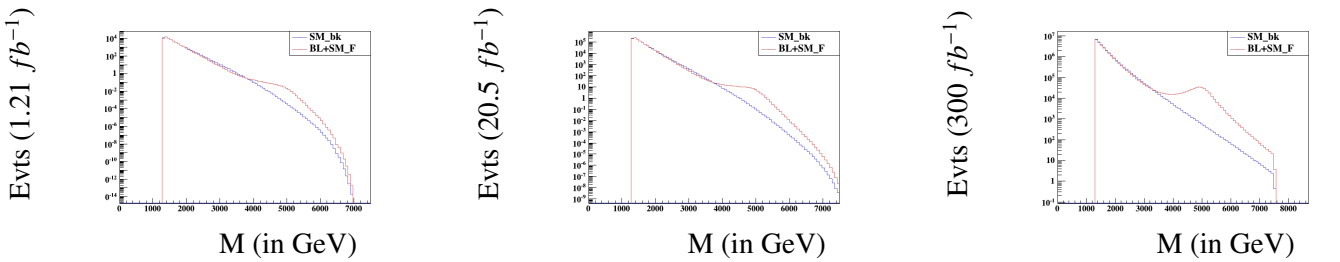


Figure 10: Dataset - F with cuts, P_T^4 , η^4 and $1306.4 \text{ GeV} \leq M_{\mu^+ \mu^-} \leq 8693.6 \text{ GeV}$ (for $\Gamma_{SW}^{signl-F}$)⁵

Acknowledgement

This study of Z'_{B-L} was carried out as a dissertation thesis of M.Sc. Particle Physics program, under the guidance of Dr Sebastian Jäger, University of Sussex, U.K. I express my sincere thanks and gratitude to my thesis adviser here.

I thank the Physical Research Laboratory (PRL), Ahmedabad for hospitality and support during which I got an opportunity to present our work in the Pheno01@IISERMohali workshop. My humble thanks to the organisers of Pheno01@IISERMohali workshop for having and supporting my stay at the IISER-Mohali, India.

The final part of this work in preparing the manuscript was done during my visiting tenure in Harish-Chandra Research Institute (HRI), India. I am extending my sincere gratitude to Prof. Biswarup Mukhopadhyaya, and the Regional Centre for Accelerator - based Particle Physics (RECAPP) - HRI for supporting me and my learning process.

References

- [1] L. Basso, [[arXiv:1106.4462 \[hep-ph\]](#)].
- [2] L. Basso, G. M. Pruna, [<https://feynrules.irmp.ucl.ac.be/attachment/wiki/B-L-SM/B-L.fr>].
- [3] J. Alwall *et al.*, JHEP **1407**, 079 (2014) doi:10.1007/JHEP07(2014)079 [[arXiv:1405.0301 \[hep-ph\]](#)].
- [4] J. Alwall, M. Herquet, F. Maltoni, O. Mattelaer and T. Stelzer, JHEP **1106**, 128 (2011) doi:10.1007/JHEP06(2011)128 [[arXiv:1106.0522 \[hep-ph\]](#)].
- [5] S. Wolfram, "Wolfram Research, Inc., Mathematica, Version 9.0, Champaign, IL (2012)," [<https://www.wolfram.com/mathematica/new-in-9/>].
- [6] L. Basso, A. Belyaev, S. Moretti and G. M. Pruna, J. Phys. Conf. Ser. **259**, 012062 (2010) doi:10.1088/1742-6596/259/1/012062 [[arXiv:1009.6095 \[hep-ph\]](#)].
- [7] L. Basso, S. Moretti and G. M. Pruna, J. Phys. G **39**, 025004 (2012) doi:10.1088/0954-3899/39/2/025004 [[arXiv:1009.4164 \[hep-ph\]](#)].
- [8] M. Carena, A. Daleo, B. A. Dobrescu and T. M. P. Tait, Phys. Rev. D **70**, 093009 (2004) doi:10.1103/PhysRevD.70.093009 [[hep-ph/0408098](#)].
- [9] C. W. Chiang, N. D. Christensen, G. J. Ding and T. Han, Phys. Rev. D **85**, 015023 (2012) doi:10.1103/PhysRevD.85.015023 [[arXiv:1107.5830 \[hep-ph\]](#)].
- [10] R. Contino, Nuovo Cim. B **123**, 511 (2008) doi:10.1393/ncb/i2008-10553-3 [[arXiv:0804.3195 \[hep-ph\]](#)].
- [11] F. Del Aguila, Acta Phys. Polon. B **25**, 1317 (1994) [[hep-ph/9404323](#)].
- [12] A. Kundu and B. Mukhopadhyaya, Int. J. Mod. Phys. A **11**, 5221 (1996) doi:10.1142/S0217751X9600239X [[hep-ph/9507305](#)].
- [13] P. Langacker, Adv. Ser. Direct. High Energy Phys. **14**, 15 (1995) doi:10.1142/9789814503662_0002 [[hep-ph/0304186](#)].
- [14] P. Langacker, Rev. Mod. Phys. **81**, 1199 (2009) doi:10.1103/RevModPhys.81.1199 [[arXiv:0801.1345 \[hep-ph\]](#)].
- [15] T. G. Rizzo, AIP Conf. Proc. **542**, 152 (2000) doi:10.1063/1.1336251 [[hep-ph/0001140](#)].
- [16] J. D. Lykken, eConf C **960625**, NEW140 (1996) [[hep-ph/9610218](#)].
- [17] T. G. Rizzo, [[hep-ph/0610104](#)].
- [18] M. Perelstein, doi:10.1142/9789814327183_0008 [[arXiv:1002.027 \[hep-ph\]](#)].
- [19] N. D. Christensen and C. Duhr, Comput. Phys. Commun. **180**, 1614 (2009) doi:10.1016/j.cpc.2009.02.018 [[arXiv:0806.4194 \[hep-ph\]](#)].
- [20] A. Alloul, N. D. Christensen, C. Degrande, C. Duhr and B. Fuks, doi:10.1016/j.cpc.2014.04.012 [[arXiv:1310.1921 \[hep-ph\]](#)].
- [21] E. Conte, B. Fuks and G. Serret, Comput. Phys. Commun. **184**, 222 (2013) doi:10.1016/j.cpc.2012.09.009 [[arXiv:1206.1599 \[hep-ph\]](#)].
- [22] C. Degrande, C. Duhr, B. Fuks, D. Grellscheid, O. Mattelaer and T. Reiter, Comput. Phys. Commun. **183**, 1201 (2012) doi:10.1016/j.cpc.2012.01.022 [[arXiv:1108.2040 \[hep-ph\]](#)].
- [23] J. Alwall *et al.*, Comput. Phys. Commun. **176**, 300 (2007) doi:10.1016/j.cpc.2006.11.010 [[hep-ph/0609017](#)].
- [24] G. Aad *et al.* [ATLAS Collaboration], Phys. Rev. Lett. **107**, 272002 (2011) doi:10.1103/PhysRevLett.107.272002 [[arXiv:1108.1582 \[hep-ex\]](#)].
- [25] G. Aad *et al.* [ATLAS Collaboration], Phys. Rev. D **90**, no. 5, 052005 (2014) doi:10.1103/PhysRevD.90.052005 [[arXiv:1405.4123 \[hep-ex\]](#)].
- [26] N. Okada and S. Okada, Phys. Rev. D **93**, no. 7, 075003 (2016) doi:10.1103/PhysRevD.93.075003 [[arXiv:1601.07526 \[hep-ph\]](#)].
- [27] Yu. Ya. Komachenko and M. Yu. Khlopov, Yadernaya (1990) Fizika V. 51, PP. 1081-1086 [English translation: Sov. J. Nucl. Phys. (1990) V. 51, no. 4, PP. 692-695].
- [28] A. Biswas, S. Choubey and S. Khan, JHEP **1608**, 114 (2016) doi:10.1007/JHEP08(2016)114 [[arXiv:1604.06566 \[hep-ph\]](#)].
- [29] M. Klasen, F. Lyonnet and F. S. Queiroz, [[arXiv:1607.06468 \[hep-ph\]](#)].
- [30] A. Alves, A. Berlin, S. Profumo and F. S. Queiroz, JHEP **1510**, 076 (2015) doi:10.1007/JHEP10(2015)076 [[arXiv:1506.06767 \[hep-ph\]](#)].
- [31] S. Banerjee, M. Mitra and M. Spannowsky, Phys. Rev. D **92**, no. 5, 055013 (2015) doi:10.1103/PhysRevD.92.055013 [[arXiv:1506.06415 \[hep-ph\]](#)].